PAPER 2009-150

Dynamic Characterization of the M19 area, Cerro Negro Field, corresponding to Carabobo Block, Orinoco Oil Belt.

A. ORTIZ.
PDVSA - E&P - ORINOCO OIL BELT DIVISION.

Abstract

Carabobo is one of the most prospective areas in the Orinoco Oil Belt with very thick sands regarding fluvial-deltaic environment with excellent petrophysical properties. This particular project was only focused on 64 square kilometers area which corresponds to a section of the reservoir containing a crude oil with average API gravity of 8º.

By integrating results from geophysics, petrophysics, sedimentology, and reservoir engineering analysis, the area was characterized with a simulation model in order to address many uncertainties which have affected the oil field exploitation since 1980. These issues are related to vertical drainage, horizontal spacing, and horizontal length to drill. Based on different simulation sensitivities were achieved the optimum configuration avoiding drainage area interference, finding also a maximum horizontal length around 4,600 feet. Moreover, there is another key factor to face about the high density of drilled wells which implies the need of looking for remaining reserves by infill drilling.

Finally, the results of this work would help to establish the optimum field exploitation scheme and reinforce the need of implementing thermal recovery projects in order to increase the primary recovery factor.

Introduction

Orinoco Oil Belt has an extension of 55,000 square kilometers, comprising Monagas, Anzoátegui and Guárico states of Venezuela. It has been divided into 4 areas, from west to east: Boyaca, Junin, Ayacucho and Carabobo (Fig 1). The assigned area of the Cerro Negro field has 120 square kilometers corresponding to the Extraheavy Oil Unit of the Morichal District, Monagas State (Fig. 2). The M-19 blocks, objective of this work, is located in the eastern.

This small section of Carabobo Block involves a STOOIP of 11,000 MMSTB approximately, having an API gravity between 7.8º and 8º. The initial reservoir pressure is about 1,200 psia and the predominant primary production mechanism is the solution gas drive. One key point to highlight is that the range of viscosities varies from 2,000 cps (undersaturated conditions) to 6,000 (dead oil viscosities). The petrophysical properties honors the fluvio-deltaic environment, therefore the average porosity is 30% and permeability might vary from 2 Darcies to 7 Darcies.

The field exploitation resides in the early 80s, beginning with the drilling of 150-300 meters spaced vertical wells within the so called experimental blocks O-16 and J-20. Further secondary recovery method (including alternate vapor injection) evaluations were conducted in order to enhance a more commercial production. In late 80s and early 90s the new uprising drilling technology was used in the area, with 400 meters spaced deviated and inclined wells where further alternate vapor injection was applied. In the late 90s and 2000s drilling campaigns of horizontal wells and multilateral wells (<2,000 feet of horizontal length) respectively were performed in the study area, observing immediately the high impact in oil production of the field. Due to the success of this technique, in late 2000s was started a massive campaign of 600 meters spaced horizontal wells of extended section (>4,000 feet) in clusters within M19 Block, noting the high oil rates as well, compared to the other configurations (Fig. 3). Nowadays, there is an average of 500 wells, highlighting that more than 80% of horizontal wells are drilled in M-19 block. As a typical heavy

oil reservoir characteristic the actual recovery factor does not exceed 3%.

Problem Statement and Scope

In despite of the previously explained and considering the low recovery factor obtained within the field, have been remaining several uncertainties about reservoir primary production mechanism, reservoir volume, fluids production behaviour, compartmentalization hypothesis and oil field exploitation scheme itself. On the other hand, it is important to clarify that, this investigation is not focused on the geological interpretation previous to the static modeling and dynamic characterization. According to that, this project was only focused to highlight the following aspects:

- Obtain a better understanding of the reservoir behaviour by integrating static and dynamic component.
- Reduce the uncertainty regarding well configuration in terms of optimum horizontal length, vertical spacing and horizontal spacing.
- Reinforce the need of implementing thermal and chemical process in order to increase the recovery factor.

Static Model

Stratigraphical Framework.

The Carabobo area is one of the most prospective areas of the Orinoco Oil Belt, mainly due to the excellent petrophysical properties and thickness of the sandstones. It is located in the Maturín Sub-basin, one of the two sectors in which the Oriente Basin has been divided. The Maturín Sub-basin (Fig. 4) is the most important petroliferous area of the Oriente Basin.

In connection to that, it is important to mention the Carabobo Block is specifically located to the eastern of the Orinoco Belt and the study area represents only 64 square kilometers. In this context the local geological description suggests in the Stratigraphic column can be identified five main events (Fig. 5), from the uppermost sequence: Mesa Formation, Las Piedras Formation, Freites Formation, Oficina Formation and the Basement. Oficina represents the formation of interest from which can be found four different members, from bottom to top: Morichal, Yabo, Jobo and Pilón.

MORICHAL MEMBER

It constitutes the main reservoir of the Oficina Formation with a high potentiality. It is formed by massive quartz sandbodies, sub angular grains corresponding to a predominant fluvio-deltaic environment having an average thickness of 450 feet. The Morichal Member (Fig. 6) from the micro scale might be sub-divided in Fluvio Deltaic Units (O-15, O-14, and O-13) and Transitional Units (O-11, O-12).

Deltaic Morichal

The lower Morichal, here named as Deltaic Morichal, is composed by fluvio-deltaic stacked sandstone bodies, mainly fluvial channel deposits, with very scarce flooding plain sediments. The average thickness for this lower section is about 200 – 300 feet. Thickness increases towards northwest. Sandstone bodies appear very thick, with very few or even none shale intercalations. This deltaic system was deposited over a preexistent irregular basement, the Guayana Shield. These irregularities in the basement were covered by the fluvio-deltaic deposits, which were developed in a kind of incised valley, which produced a huge limitation for lateral migration of the channels.

Transitional Morichal

On top of the previous units, the influence of the marine environment starts being more important, and Transitional Morichal is deposited. This section is more characteristic of a High Stand System Tract, with deposits of marine bars, shoreface, prodelta, etc. The sandstones of this level are badly connected and there is an increase in the proportion of shales to sandstones, with an approximate total thickness of 150 feet.

YABO MEMBER

Marine conditions were reached in the whole area, and the shaly Yabo Member was deposited on top of the Transitional Morichal. These units are characterized by thick sections of shales intercalated with very few levels of sandstones. The environment of deposition is from near shore to open marine. These deposits can act as seal for the underlying sandstones (Morichal Member) and have an average thickness of 250 feet.

JOBO MEMBER

It is constituted by fluvio deltaic character and the same time represents the second reservoir of the Oficina Formation, whose sedimentation began after marine transgression of the Yabo Member. This depositional regime finishes with other transgression.

PILON MEMBER

According to the sequence this member was deposited, immediately after the transgression. It is essentially constituted by a shaly character with a very few percentage of sandstone.

Structural Framework

In first instance the structural model was based on the interpretation of two 3D seismic cubes with an excellent covering of 116 square kilometers which surpass the study area. From this information was possible to interpret two key seismic reflections having a high acoustic impedance contrast. These surfaces correspond to Pilón Member and Basement. On the other hand, the area counts with more than 15 seismic logs, guarantying the time to depth conversion reliability. In this context the main interpretation of structure describes a monocline gently deepening towards the NE (Fig. 7) with an angle of about 1°- 3º. The basement is crossed by several sub-vertical faults having a general east to west trend (Fig. 8). The vertical displacement vary from 50 feet to 120 ft, encountering sand bodies in both sides of the faults which allows to hypothesize the no sealing character due to the massive sand packages. A further detail will be given in the pressure model.

Horizons Definition and Gridding.

In order to achieve the structural and stratigraphy integration was used 139 interpreted wells with their respective tops corresponding to the five litoestratigraphic units (from O-11 to O-15) and the interpreted surfaces from seismic. Additionally, main faults were taken into account to counteract a significant impact during the horizontal wells drilling. Five Horizons were

generated by using the convergent interpolation algorithm and the results can be noted in the figure 9; highlighting the fact that the fluvio-deltaic horizons were conformed to the basement and the transitional ones were conditioned to the uppermost strata.

Moreover, the gridding process was achieved considering the following aspects:

- Available resource.
- Main geological features.
- Purpose of the modeling.
- Counteract upscaling.

In first place, the resource is referred to the capacity of the computer to handle the data and process it. During the modeling will be carried out the using of robust algorithms and different flow equations (Material Balance and Darcy's Law) which requires high computer performance in order to reduce response of many outputs. In addition, another key issue resides on capturing the main geological features such as: main facies, major faults, vertical and horizontal barriers and so on. In this particular case, it is convenient to point out the presence of some vertical barriers which were reflected in the static pressure measurements in some wells within the study area, getting a thickness between 10 ft – 15 ft (Fig. 27). As can be noted, the oil gradient line presents disruptions coinciding with some interbedded shales across the stratigraphic sequence, this is a clear evidence of vertical compartmentalization. From this point, it is important to clarify, this behaviour was visualized in some sectors of the reservoir, therefore it not a regional character.

Secondly, the purpose of the modeling is extremely related to the previous facts, since it results important to keep in mind the aspects that investigator wants to address; from this it can be selected (corner point grids, cartesian grids, radial grid and so on). This project looks forward to getting a dynamic model; therefore a very fine gridding is not needed. As a result, by building a not extremely fine grid, it might be counteracted the effects of upscaling in order not to wash out the heterogeneities.

Finally the gridding was established having a static model of 1,173,060 cells (126 x 98 x 95) (Fig. 10) with the following dimensions: X=12,565.61 mts, Y=9,867.57 mts, Z=1,250 ft. Meanwhile, the spatial resolution is given by Dx=100 mts, Dy=100 mts and Dz=13 ft.

Sedimentological Modeling

As was previously described in the stratigraphy, the sedimentological framework in the Morichal Member is characterized by the fluvio-deltaic domain and a transition to a marine environment. This information is supported by the interpretation of 139 electrical logs and the analysis of three core samples (1,324 feet) which were taken from three different wells dispersed within the whole study area. This information allowed confirming that Pilón Member along with Yabo Member represent maximum flooding surfaces (MFS), involving transgression periods. The facies interpretation suggests the presence of distributaries channels in the lowest massive sand packages (fluvio-deltaic environment) and the proportion decreases in the transitional environment in which increase the floodplain shales and point bars presence. From this information, facies codification[3] and the extrapolation of the discrete variables were carried out by using Sequential Indicator Simulator (SIS) algorithm, through specialized software. In first place, previous to extrapolation, this algorithm envisages two major steps: log upscaling and the adjustment of the variograms.

Log upscaling process is necessary to average data according to the establishment of vertical gridding; since it is being dealt with discrete variables, was used the most of as an upscaled technique. The consistency of the results can be seen in figure 11.

On the other hand a reticent step is the adjustment of the variograms in order to define the degree of spatial correlation amongst the discrete variables. It is important to point out; the variograms were biased to a previous interpreted model by a sedimentologist and using a trial-error process to get the best direction for spatial correlation. In connection to this, it was observed the huge correlation range, from the statistical point of view, of the fluvio-deltaic channels which reflects the domain of this facie within the reservoir. Following a similar procedure the variograms for every facie corresponding to the five litoestratigraphy units (15 variograms) were fixed (Fig. 12, 13, 14, and 15).

Petrophysical Modeling

The input data from the petrophysical modeling consisted in the same 139 interpreted well logs, having conventional petrophysical curves such as: effective porosity (PHIE), permeability (Perm), shale volume (Vsh), and water saturation (Sw). The net to gross ratio was determined as a function of shale volume (Fig. 16) by an estimated equation from the data analysis.

NTG = -1.0575*Vsh+0.9728……...……...Equation (1)

The modeling process, as was previously described, implied log upscaling and the adjustment of the variograms for every property in order to define the spatial correlation (Fig. 17, 18, 19). The petrophysical modeling was biased to the facies model by using the sequential gaussian simulator (SGS) algorithm. Even though this procedure was realized in order to guaranty the consistency in the prospective and non-prospective zones with channels and floodplain respectively, it was necessary to define some shale cut-off regarding the minimum (0.02) porosity and permeability (0.06 D) otherwise the property extrapolation would be misleaded. The results of the modeling can be visualized in figure 20.

Upscaling to simulation

In the gridding section were discussed the main issues about the selection of the suitable grid for modeling. In this opportunity one of the main aspects encompasses the capacity of the computer to handle million of cells. In order to improve the performance of the computer without sacrificing geological features, the upscaling of the grid was made considering the same vertical resolution (13 ft) and the correlation length reflected by the variograms for the major and minor directions. Therefore, the model for dynamics purposes has 195,510 cells (40 x 49 x 95) where the spatial resolution is given by Dx=300 mts, Dy=200 mts and Dz=13 ft (Fig. 21).

Volumetric Estimations

For the estimations of the oil and gas originally in place were considered the gross rock volume given by the 3D model, the extrapolated petrophysics and basic PVT data such as: Boi (1.0812 Rb/Stb), and Rsi (106 Scf/Stb). By using the equation 2

and 3 the STOIIP and GIIP were finally calculated, mentioning that 4 sensitivities were carried out with the initial water saturation according to the analysis of the logs and the data obtained from cores.

STOIIP = [7758*Φ*(1-SWI)*GRV*NTG]/ Boi……..Equation (2)

GIIP = STOIIP*Rsi.……...Equation (3)

The volumetric results are shown in table 1, where the definitive figure were taken from a lognormal distribution as 10,957 MMStb and 1095.7 MMMScf values were taken as representative of the oil and gas reservoir volume respectively.

Dynamic Model

Rock Fluid Model

For the rock fluid model was used the available data from electrical logs and two cores samples (CIB0006E and CIB0007E) which were acquired within the study area. The analysis and identification of the rock types was based on global hydraulic elements (GHE) methodology proposed by Corbett and Potter in 2,004 which represents a regular progression of the rock quality index (RQI) and flow zone indicator (FZI) concept proposed by Amafeule et. al in 2,003. This new approach proposed the use of pre-determined template on which are built a series of GHE based on classical FZI values covering a wide range of possible combination between porosity and permeability values. These FZI values determine the boundaries amongst the rock types.

$$RQI = 0.0314 * \sqrt{\frac{K}{\phi_e}} \quad \text{……Equation (4)}$$

$$\phi_z = \left(\frac{\phi_e}{1-\phi_e} \right) \quad \text{……..Equation (5)}$$

$$FZI = \frac{RQI}{\phi_Z} \quad \text{……...Equation (6)}$$

Obtaining K from equation 4, and substituting 5 and 6:

$$K = \phi * \left[\frac{\left(FZI * \left(\frac{\phi}{1-\phi} \right) \right)}{0.0314} \right]^2 \quad \text{……..Equation (7)}$$

According to the equation 7 for a given porosity value and the pre-established FZI (table 2) the permeability can be calculated, therefore these values are plotted in order to define the GHE template. Once the template was built, the core data was plotted on it allows us to identified four main rock types (Fig. 22). The rock type four was considered as a non-reservoir rock since the permeability values are lower than 100 mD, in accordance with the petrophysical cut off determined in previous studies.

However, taking into account the special core data it is imposed the need of making a subdivision of the rock types by analyzing the capillary pressure and relative permeability end points. The analysis shows that between the FZI classes (GHE) it might be found in some plugs different irreducible water saturation and residual oil saturation values. This envisages a wide grain size variation amongst the macro rock type established with global hydraulic elements.

Another key feature to point out is the wettability analysis made by obtaining amott test results (Fig. 23) which reflects that the predominant condition seems to be intermediate to oil wet. This issue, it is quite consistent with the field production behaviour because of, when occurs water breakthrough into the wells the increase in the water rate is extremely abrupt and the oil production decline quickly. Moreover, the mobility ratio is so unfavorable to the oil, comparing thousand of centipoises against centipoise units.

In agreement, it was established seven rock types which are shown in table 3. The laboratory relative permeability curves were adjusted and smoothed in order to avoid some numerical problems and monotonicity errors during simulation, for this procedure was used the Corey equations. On the other hand, it was also necessary to generate relative permeability data for some rock types by using numerical regression models[5], Burdine and Purcell equations. The definitive relative permeability (water-oil / gas-oil) curves can be visualized in figures 24 and 25. For simulation purposes the capillary forces were ignored due to the fact that in heavy oil reservoirs the viscous and gravitational forces dominate the flow, moreover in the macro scale (coarse models) the effect of capillary forces become almost negligible.

Pressure Model

In terms of the pressure model it was taken into account and validated all information available until 2007 about 350 BHT-BHP data, 50 static fluid levels 14 static pressure measurements and the information for 30 horizontal wells with permanent pressure gauges.

BHT-BHP Measurements

The static BHT-BHP measurements were taken in static conditions and consist in getting down a pressure gauge then it is positioned in front of certain depths for a specific time periods in such a way to acquire pressure and temperature values at the desire points. This data allow inferring the average static pressure of that well.

In order to guaranty the reliability of the pressure model these data was validated according to the following criteria:

- Pressure point affected by recent huff and puff cycles (high temperature).
- Values which present abnormal pressure gradient considering the oil and water densities of the reservoir fluids it means lower than 0.4091 psia/ft and higher than 0.56 psia/ft respectively.
- It was considered the measurements captured nearest from sand face within the borehole.

Following the previous procedure 183 points were validated and the rest were dismissed. Then, these points were normalized to the reservoir reference depth (-2,700 Tvdss) by using the fluids gradient and the equations 8, 9 and 10.

$$Tvdss_{SF} = \left(\frac{D1 + D2}{2} \right) \quad \text{……...…….Equation (8)}$$

$$Wbhp_{SF} = Wbhp_{P} + \Delta_{WF} * (Tvdss_{SF} - Tvdss_{P}) \quad \text{……..…..Equation (9)}$$

$$Wbhp_{D} = Wbhp_{SF} + \Delta_{RF} * (Tvdss_{D} - Tvdss_{SF}) \quad \text{…..……..Equation (10)}$$

Pressure Gauge Measurements and Static Fluid Level

Another source of pressure information is represented by the pressure gauge measurements from permanent downhole gauges and static fluid levels. Firstly, the data considered from the permanent gauges was obtained before activating the wells in order to ensure static conditions and get a better estimation of the static average pressure within the near wellbore region. Therefore, all the data was also normalized to the reservoir datum by using a similar procedure.

Static Pressure Measurements (RFT Data)

By analyzing the static pressure profiles for the 14 wells, it was determined an average oil gradient between 0.4080 and 0.4090 which represents typical values for heavy oils. In connection one key point to highlight is the fact that, the independent analysis for each well, located in different sectors of the study area (Fig.26), reveals similar oil gradients which is a clear indication of the same type of fluids; therefore there might not be a compositional variation among and across the whole reservoir.

On the other hand, another key aspect, it is represented by the disruption in the oil gradient line at certain depths, hence reflecting an indication of vertical compartmentalization in some sectors within the reservoir (Fig.27). Observing this figure, it is realized these disruptions correspond to interbedded shales which might represent local seals or barriers in the stratigraphic column.

In accordance, by taking a look of the structural framework within the whole area, it has been using a sub-division in three different reservoirs (OFIM CNX 9, OFIM CNX 24 and OFIM CN 42) based on the fact of having sealing faults. However, there are some important aspects which might conduct to the opposite hypothesis:

- Despite that the huge fault throws (80-100 ft), the massive sand packages (200-300 ft) counteract them, which allow thinking hydraulic communication in both sides of the fault planes.

- According to the explanation in the paragraph 1, there is an evidence of the same fluid type in the whole area. This is supported by an average API estimation which was made with the wells completed in each block. The estimation reflects similar API gravities (7.8 -8.1 API) in the three blocks.

- The pressure-depth points (oil gradient lines) for the three blocks were plotted, visualizing the same pressure trend in OFIM CNX 24 and OFIM CN 42 reservoir, and a small difference (20 psi) with the OFIM CNX 9 reservoir (Fig.28). This can be attributed to the fact that the fluids cumulative production of the OFIM CNX 09 is the lowest, which suggests a high energetic level.

As a consequence of all the issues explained above the pressure model was built, reflecting an initial reservoir pressure of 1,230 psia and current average pressure of 900 psia (Fig. 29). Finally, due to the modeling was made in only 64 km^2 of the reservoir area, it was necessary to realize a pressure model for this sector, emphasizing this block has been less drainage than the rest of the reservoir area; as a result the current sector average pressure is about 1,150 psia.

PVT Model

In order to guaranty the consistency of the PVT data available is necessary to validate the basic parameters such as °API, temperature (T) and initial solution gas to oil ratio (Rsi). In first instance, the API estimation consist of collecting the data regarding the API values per well determined during the first five years of production and hence by using a frequency histogram it was estimated a range between 7.8– 8.1, validating the average °API (8) of the reservoir. For the reservoir temperature was used temperature profiles obtained in 14 well (RFT data) from which was determined a normal temperature gradient of 0.0110 °F/ft. As a result, taking into account a mean surface temperature of 88 °F and the Datum (-2,700 Tvdss) the average reservoir temperature was estimated about 119 °F. In terms of Rsi was made a cumulative oil production against producing GOR (Fig.30) graph, noting stabilization in the initial GOR between 90 Scf /Stb and 110 Scf/Stb.

Based on the above, it was made a collection of 18 PVT tests within the Cerro Field having 16 recombined samples and 2 bottom samples (table 4). By checking consistency with the basic parameters only 4 PVT tests were consistent. Therefore, it was applied the basic validation criteria in terms of Linearity of Y Function, Mass Balance and Density estimate; resulting these 4 PVT test were not representative of the reservoir fluid properties, observing average errors higher than 10% (Mass Balance) in most of the cases.

However, there are some important aspects to spot within the 18 PVT samples, and is related to the fact that 3 PVT test (corresponding to the well CI0210) honors the linearity of the Y function, indicating a good estimation of the bubble point pressure. Even though they were realized at higher temperature (129°F) than the reservoir conditions (119°F) and considering that small changes in temperature does not produce dramatic changes in the bubble point pressure, it might be gotten a gross magnitude of the bubble point; having 705 psia as the pseudo bubble point and 1,100 psia as the bubble point . This range of values suggests that the foamy oil phenomenon is presented within the reservoir; this issue will be addressed in the history matching process.

Finally, it was necessary to generate synthetic PVT using correlations proposed by PDVSA-INTEVEP[4] in which they considered a wide range of heavy oil PVT samples around Venezuela's oil basins. For water properties were used McCain and McCoy correlations. The results of PVT properties are presented in the figures 31, 32, 33 and table 5.

Material Balance Calculations

As Dake points out material balance represents a very powerful tool to get the first insight of the reservoir behaviour prior to carry out a numerical simulation. In this case by the help of specialized software based on Havlena-Odeh technique material balance was performed. Thereby, validated production behaviour, pressure model and PVT properties were uploaded into software and different scenarios were studied and analyzed.

Base Case (Non-Aquifer/ Non-Gas Cap)

The base case corresponds having a reservoir without the influence of an extra-energy support (gas-cap / aquifer). By the visualization of the figure 34, it can be noted that reservoir production is not supported at all by depletion; hence the so called Campbell plot (Fig. 35) might confirm the presence of an extra energy support which does not contribute significantly to the pressure maintenance. Due to the characteristics of this undersaturated reservoir, there is not an original gas-cap but there is an evidence of an oil-water contact towards the north of the structure (Fig. 36) in the deepest section of the reservoir (-3,180 Tvdss), this hypothesis is confirmed for the water production of the wells, located to the north. Therefore, it is quite logical to infer the presence of a finite aquifer by analyzing the shape of the curve, where later in production there is less support from the aquifer.

Case 1 (Finite Aquifer)

Based on the above, it was tried to match the aquifer parameters using different finite aquifer models in order to reproduce the production history as a function of pressure. However, the result reflects the non-uniqueness of the final outputs since it was found an apparent match with two different models and aquifer parameters such as: Carter Tracy (Radial) and Fetkovich (Semi-Steady State / Bottom Aquifer). From the quantitative point of view, it is not reliable to spot result as definitive, these models suggest lower oil in place than the volumetric calculations which might imply a quality check and validation of the petrophysical cut off to estimate net-pay.

Nevertheless the non-uniqueness of the results resides on the uncertainty associated to the aquifer parameters such as: aquifer volume, encroachment angle, aquifer permeability, aquifer ratio and so on. In addition, the different aquifer models suggest idealization criteria of the reservoir dimensions which sometimes results extremely difficult to approximate the reservoir shape to a circle or a cube.

On the other hand, the basic principle of material balance envisages that the reservoir behaves like a tank, where the pressure disturbance diffuses fast throughout the reservoir and pressure equilibrates immediately. In this case, it is being dealt with an extra heavy oil reservoir whose hydraulic diffusivity constant results very low due to the high viscosities which might limit the material balance application in this type of reservoirs.

Finally, for the purpose of this investigation it concludes the material balance results will be considered from the qualitative point of view instead of quantitative.

Numerical Simulation

The numerical simulation was performed characterized for a black oil model by the help of specialized software. The first step was based on data importing to the simulation software in which was uploaded the Static model (grid, petrophysical model, faults and producer wells), pressure model, PVT properties, rock-fluid model, validated production history and the well events (workovers, services and interventions). Secondly, with all data uploaded, the initialization process was made in order to verify equilibrium conditions within the reservoir, confirming in this case the initial pressure of 1230 psia. The oil water contact depth was established at -3180 Tvdss.

HISTORY MATCHING

By the integration of the static and dynamic component the history matching process was executed in order to reproduce the fluids production (oil, water and gas). In first place the pressure response reflects a satisfactory match with the pre-established pressure model (Fig.37), highlighting there is an agreement with material balance results since it was not necessary to model an aquifer due to the low contribution for the pressure maintenance. In connection, the oil volume results (figure 38) show a very good match throughout the field history, which confirm that petrophysical model and oil PVT properties, honors successfully the oil production behaviour.

For water production, it was gotten a moderate match of the fluid volumes (Fig.39). As was previously described in the rock fluid model, the reservoir wettability seems to vary from intermediate to oil wet and this variation came from different special core analysis (taken in different wells) which might suggest a wettability variation within the reservoir. Additionally, there is an uncertainty related to the lab procedure itself to generate relative permeability curves due to the usage of lower viscosity fluids to simulate the fluid flow through the porous media. As a consequence, all these issues affect directly water production match. However, in the water production match the key point was the critical water saturation which was higher than 10% in the rock fluid model. This parameter was adjusted after several trials with the simulator.

Regarding gas volumes, it was found a quite satisfactory match since the simulated data is closer to the historical gas rates (Fig.40). In first place, in order to achieve the production match, it was necessary to adjust the bubble point pressure to 1,100 psia rather than the so called pseudo bubble point pressure. Secondly, the critical gas saturation within the rock fluid model was fixed in 3%, after several runs. From these key aspects, it stands out a paradigm about the presence of the foamy oil phenomena in this reservoir because of one bottom hole PVT sample (CI0210 well) reflects a re-marked difference between the conventional and non-conventional test in terms of bubble point figures which indicate a pseudo bubble point in 700 psia. In accordance, a depletion test was carried out estimating critical gas saturation values from 8% up to 24%, however the model contradicts this point marking the need of reducing this values to reproduce the gas movement through the porous media.

SENSITIVITIES

Once the history match was achieved, it might be inferred that all properties are consistent with the model and hence different sensitivities about horizontal spacing, vertical spacing, and horizontal length were performed. In order to do this one area of the reservoir was selected, specifically in the lower layers within the fluvial-deltaic environment having excellent petrophysical properties. Various scenarios were set and forecasted until 2,030.

Horizontal Length

It was built an artificial horizontal well in the sector mentioned above by generating different cases varying the horizontal length from 2,000 to 6,000 feet and considering a constant pressure drop of 200 psia. According to the results (figure 41) is shown a quite logical response about the oil rate since is observed that the longer the section the higher the oil rate (at the same pressure drop) until is reached more than 3,000 feet in which the oil rate stabilize. From this point the oil rate remains almost constant until certain period depending on the

section length. If it is observed the figure 42, it is ratified the previously explained but it can be noted a theoretical limit close to 4600 feet due to the oil cumulative production does not present major variations between 4600 and 6000 feet. The reasoning of this results are based on the friction forces along the horizontal section which increases as the horizontal length augment, therefore there will be some section of the horizontal length that will not contribute to the flow (generally the section nearest to the toe).

Horizontal Spacing

For the horizontal spacing, it was adjusted a typical cluster's well row varying the horizontal distance between the branches beginning with 600 mts up to 150 mts. The cases are conformed such as follow: two wells spaced at 600 mts (Case 1), three wells spaced at 300 mts (Case 2), four wells spaced at 200 mts (Case 3) and five wells spaced at 150 mts (Case 4).

The cases were simulated into the numerical model, showing (figure 43) in first place for the two wells spaced at 600 mts a lower cumulative production. From this point the cumulative production starts to increase until certain limit, represented for the case 3 in which the cumulative production is quite similar to the previous case and tend to be even lower. This might be explained by the fact that, the closer the spacing the higher is the interference and hence the pressure decrease quicker, achieving the bubble point and accelerating gas liberation and the consequent gas production. In other words, if the relative permeability to gas increases the oil flow decreases.

Finally it may be hypothesized, that the drilling of five wells spaced at 150 mts would not increase oil production rather than gas production (Fig. 44); suggesting in this case a maximum of 4 wells spaced at 200 mts.

Vertical Spacing

The sensitivities were done following a similar procedure in the same sector of the reservoir by placing the wells at various positions starting from 10 mts up to 100 mts. In this way, all the cases were generated and compared to a base case positioned at the bottom of the sand. In order to verify vertical interference, the reference well was virtually activated 6 months prior to the activations of the other well. In the figure 45 it can be pointed out two main issues. The first observation is based on the activation of the other well 6 months after the reference well, it is noted in all the curves that the static pressure tend to decrease quicker from this moment. The second observation corresponds to a quite logical response where, the closer to reference well, the higher is the vertical interference and the static pressure diminishes faster. In addition, it can be observed, when the wells are vertically spaced between 80 ft – 100 ft the interference tends to decrease. In the analysis mentioned above the permeability vertical anisotropy plays an important role in the vertical drainage of the horizontal wells, due to the characteristics of the described fluvial-deltaic environment this value tend to be higher than 0.6 in clean sandstones.

FORECAST

The final stage of this investigation encompasses the simulation of different scenarios in order to address the optimum exploitation scheme applying conventional process by drilling horizontal wells of 4600 ft length (cold recovery). According to the sensitivities, it was established 4 different cases such as:

- Base Case: Merely, energetic decline.
- Case 1: Drilling 60 wells horizontally spaced at 600 mts
- Case 2: Drilling 80 wells horizontally spaced at 300 mts.
- Case 3: Drilling 120 wells horizontally spaced at 200 mts.

Firstly, the results showed in figure 46, reflects an energetic decline of 5%, involving a recovery factor of 5% in 20 years. The other cases were compared, and it can be visualized an increase in the recovery factor from the case 1 to the case 3. Therefore, the horizontal spacing reduction will augment the recovery factor from the actual scheme 6.5% to 9% (Fig. 47); the increase seems to be low due to the characteristics of this heavy oil reservoir. Moreover, this figure might represent a theoretical limit in cold recovery and the same time reinforces the need of applying thermal process in order to increase significantly the oil field recovery factor.

Conclusions

- According to the pressure model it was not detected the evidence of main compartments within the reservoir.
- The main primary production mechanism is dominated by solution gas drive.
- The petrophysical properties and fluid model honors the production behaviour of the whole field.
- The critical gas saturation in order to achieve the production gas match was 3% approximately.
- During the first years of production the horizontal wells would not result affected by the energetic decline.
- The optimum horizontal length should not exceed 4600 feet.
- Vertical drainage suggests 80 ft of spacement in order to minimize interference.
- The cold recovery factor would increase by reducing the horizontal spacing up to 200 mts.

Acknowledgement

I would like to acknowledge to PDVSA E&P – Orinoco Oil Belt Division for the permission to present these results. Thanks are extended to the Reservoir Management of Morichal District and my colleagues from Plan and Reserves section for supporting me in the realization of this investigation.

NOMENCLATURE

°API	=	API Gravity (Oil density unit)
psia	=	Absolute pound square inch (Pressure unit)
D	=	Darcy (permeability unit)
mts	=	meters (length unit)
ft	=	feet (length unit)
Boi	=	Initial oil formation volume factor
Bo	=	Oil formation volume factor
Rsi	=	Initial solution gas to oil ratio

Rs	=	Solution gas to oil ratio
GOR	=	Gas oil ratio
Bgi	=	Initial gas formation volume factor
Bg	=	Gas formation volume factor
Stb	=	Standard condition barrels
Scf	=	Standard cubic feet
Rb	=	Reservoir condition barrels
Grv	=	Gross rock volume
ϕ	=	Porosity
K	=	Permeability
Vsh	=	Shale volume
Ntg	=	Net to gross ratio
STOIIP	=	Stock tank originally oil in place
GIIP	=	Gas originally in place
GHE	=	Global hydraulic element
FZI	=	Flow zone indicator
BHT	=	Bottom hole temperature
BHP	=	Bottom hole pressure
W	=	Well
Tvdss	=	Sub-sea true vertical depth
D	=	Datum (Reference depth)
P	=	Depth of the pressure measurement
D1	=	Top of the completed sand
D2	=	Base of the completed sand
SF	=	Sand face
Δ_{WF}	=	Well fluid gradient
Δ_{RF}	=	Reservoir fluid gradient

REFERENCES

1. Useche, F., Bejarano, C., Didanloo, A., and Shahbazian, S., Integrated Rock Properties and Fluid Distribution Determination Using Core and Log Data, Oficina Formation, Ayacucho Area, Orinoco Oil Belt, *Paper 2008-462, II World Heavy Oil Congress, Edmonton-Canada, March 2008.*

2. Ortiz, A., Del Saz, M., Guerello, R., Paz, J., and Elmadhouni, A., Orinoco Oil Belt Project: M19 Development Plan; *project presented in partial fulfillment of the requirements for the degree of master of science in oil and gas engineering at Instituto Superior de la Energia (ISE), Madrid- Spain, July 2007.*

3. Figueroa, H., Perfecto, Z., Contreras, A., and Benitez, F., Stratigraphical and Sedimetological Description of the Cerro Negro Field; *project presented in PDVSA reservoir conference, Monagas-Venezuela, December 2007.*

4. Hener, C., Lago, M., and Perez, V., Evaluation and Generation of PVT correlations for Venezuelan's Heavy Oils, *technical report presented by INTEVEP as a requirement of PDVSA E&P, Miranda-Venezuela, October 2001.*

5. Mohamad, I., and Koereditz, L., Two Phase Relative Permeability Prediction Using Linear Regression Model, *SPE 65631, SPE Eastern Regional Meeting, West Virginia-USA, October 2000.*

6. Huerta, M., Mirabal M.C., Ring, W., Treinen, R., and Spence, A., Hamaca: Solution Gas Drive Recovery in a Heavy Oil Reservoir, *Experimental Results, SPE 39031, Fifth Latin American and Caribbean Petroleum Engineering Conference and Exhibitions, Rio de Janeiro-Brazil, September 1997.*

7. Rodríguez, H., Vaca, P., Gonzalez, O., and Mirabal M.C., Integrated study of a heavy oil reservoir in the Orinoco Belt: A Field Case Simulation, *SPE 38015, Reservoir Simulation Symposium, Dallas-USA, June 1997.*

Appendices (Figures and Tables)

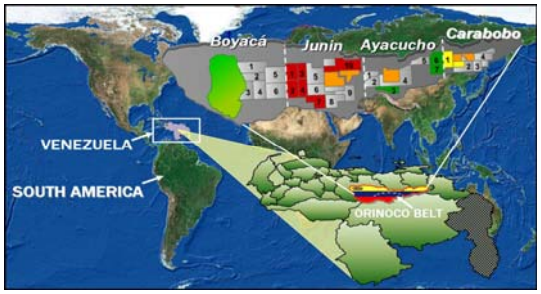

Figure 1. Orinoco Belt Geographic Location.

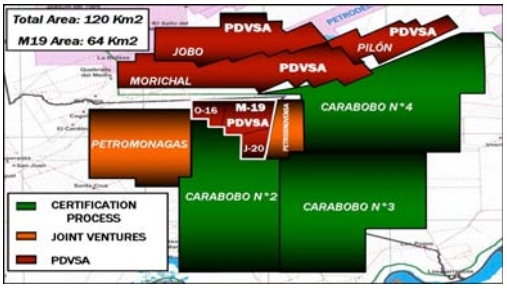

Figure 2. M-19 Block Geographic Location.

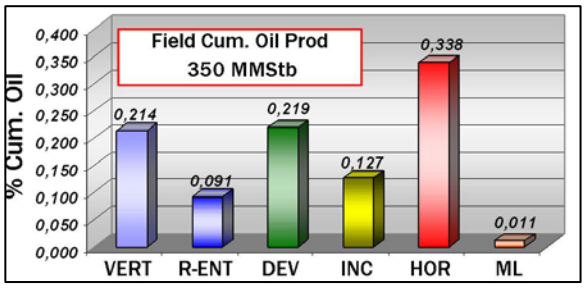

Figure 3. Well configuration contribution to oil production.

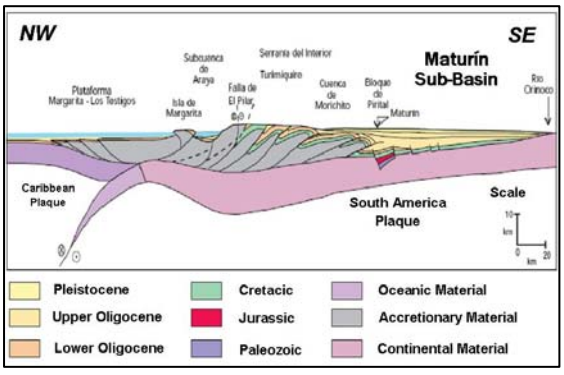

Figure 4. Regional Cross-Section in Eastern Venezuela.

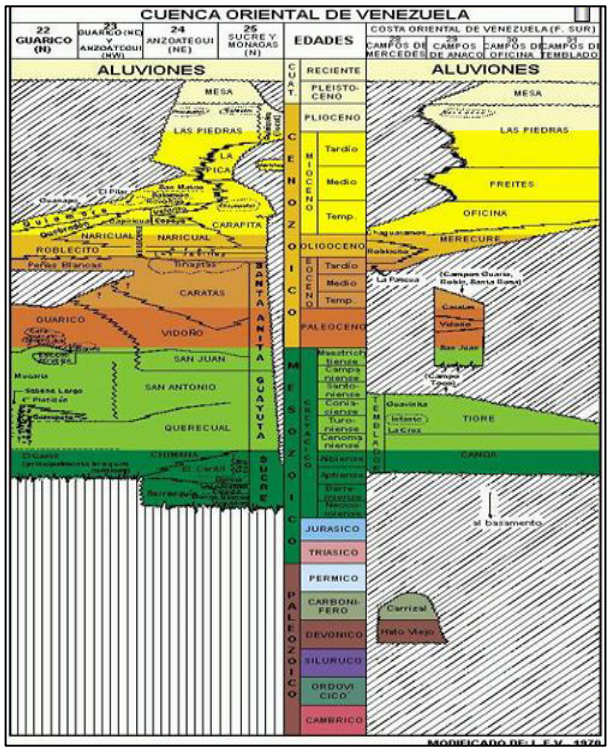

Figure 5. Regional Stratigraphic Column of Oriente Basin.

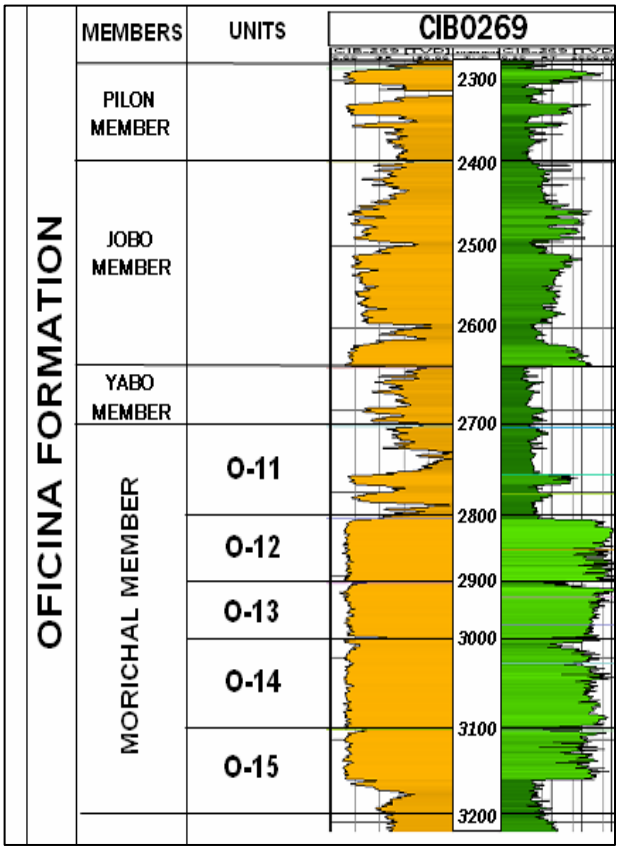

Figure 6. Stratigraphic Column of Cerro Negro Field.

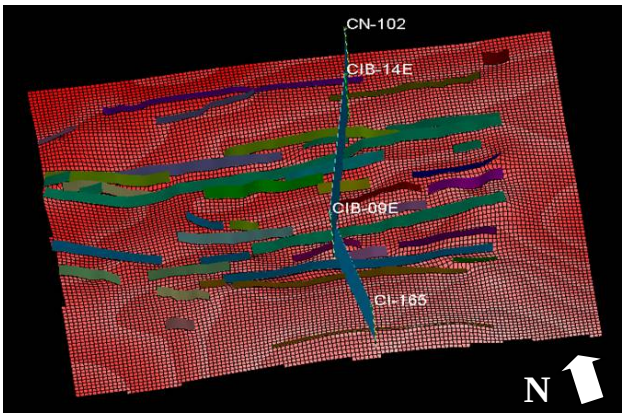

Figure 7. Structural Framework of M-19 Block.

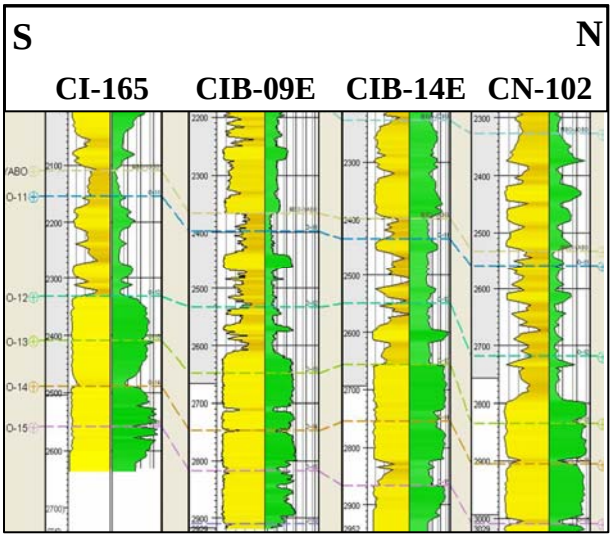

Figure 8. North - South Structural Cross Section.

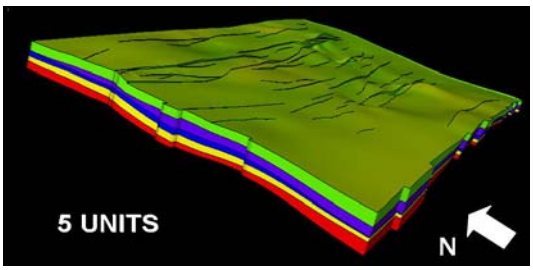

Figure 9. Stratigraphic and Structural Integration.

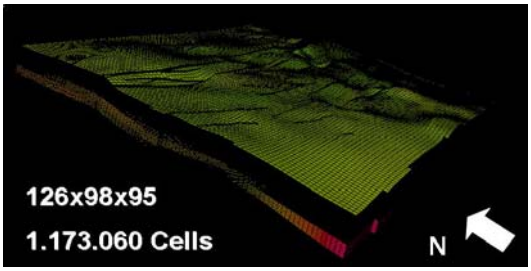

Figure 10. Horizons and Gridding Definition.

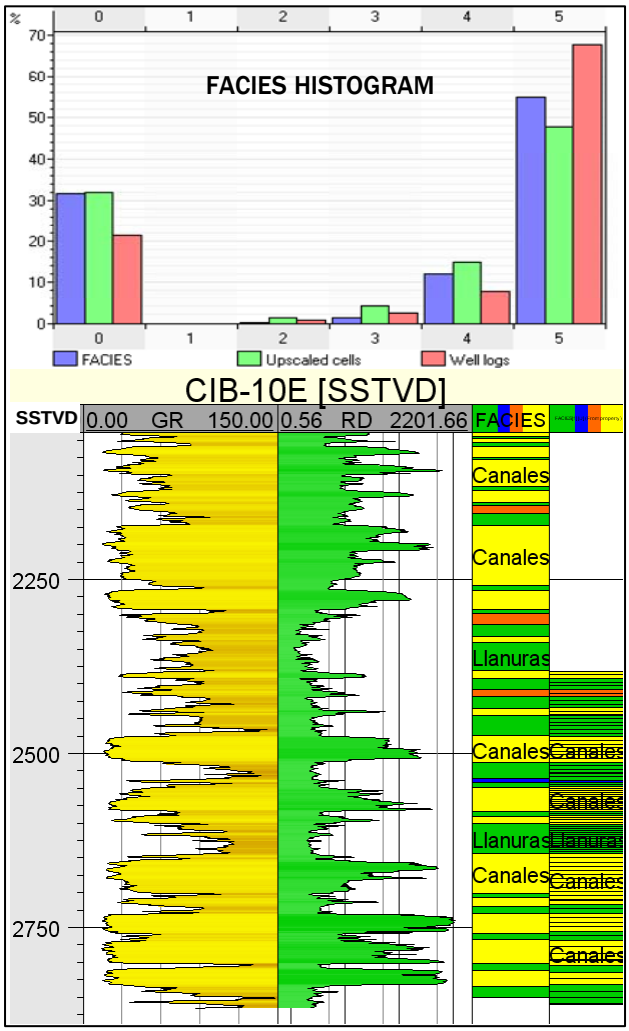

Figure 11. Horizons and Gridding Definition.

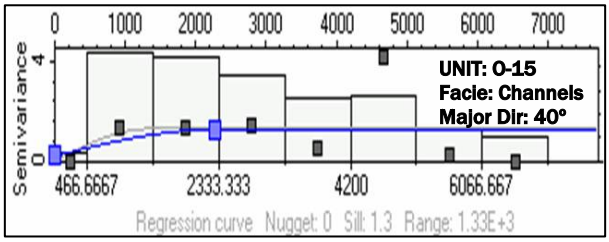

Figure 12. Variogram for fluvial channels of the O-15 Unit.

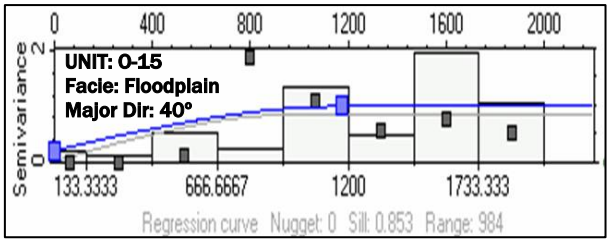

Figure 13. Variogram for floodplain of the O-15 Unit.

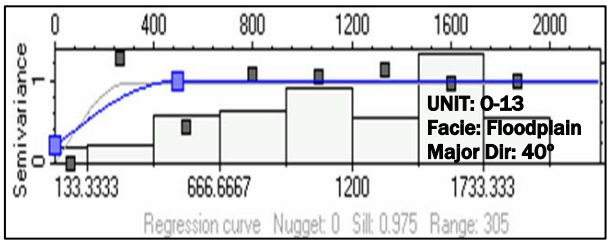

Figure 14. Variogram for floodplain of the O-13 Unit.

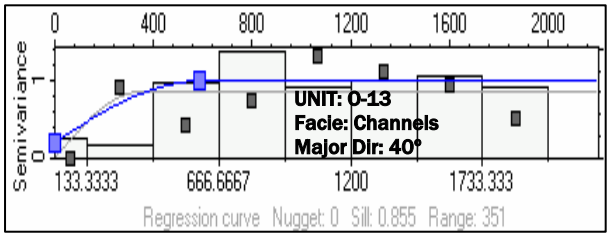

Figure 15. Variogram for fluvial channel of the O-13 Unit.

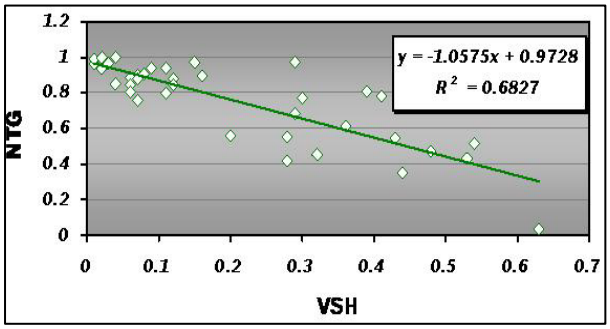

Figure 16. Shale volume-Net to gross relationship.

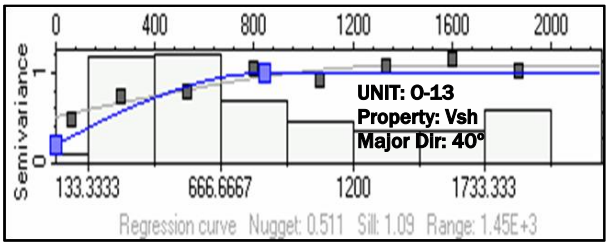

Figure 17. Variogram for shale volume of the O-13 Unit.

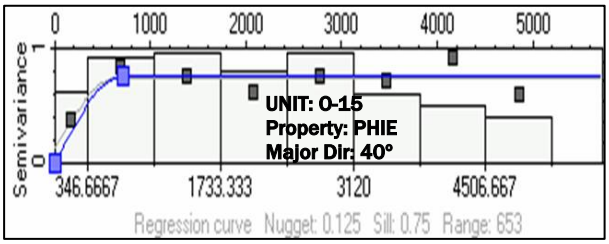

Figure 18. Variogram for porosity of the O-15 Unit.

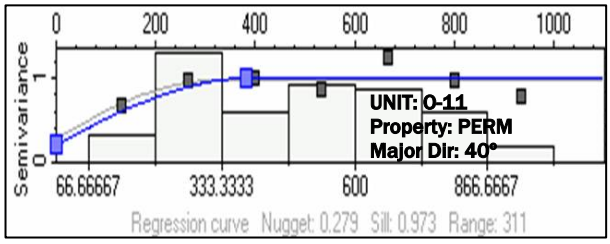

Figure 19. Variogram for permeability of the O-11 Unit.

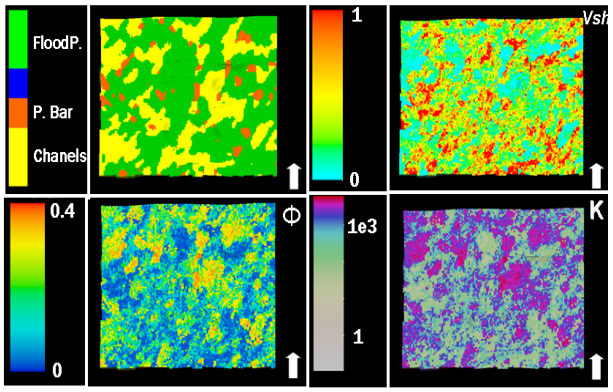

Figure 20. Facies and Petrophysical Model (O-11 Unit).

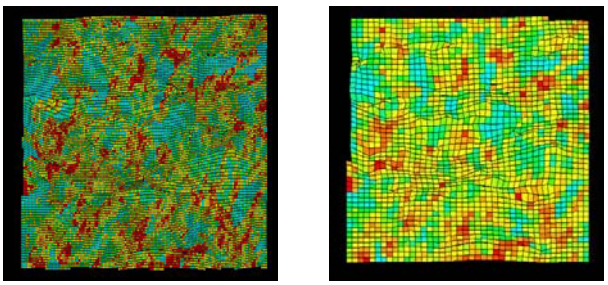

Figure 21. Upscaling. (A) Fine model. (B) Coarse model

Cases	Description	STOOIP (MMStb)	GIIP (MMMScf)
1	Swi = 0,07	12583	1258,3
2	Swi = 0,17	11230	1123
3	Swi = 0,29	9606	960,6
4	Swi = 3D Model	10619	1061,9

Table 1. Sensitivities STOIIP and GIIP of M-19 block.

FZI	GHE
48	10
24	9
12	8
6	7
3	6
1,5	5
0,75	4
0,375	3
0,1875	2
0,0938	1

Table 2. Pre-established FZI values representing GHE.

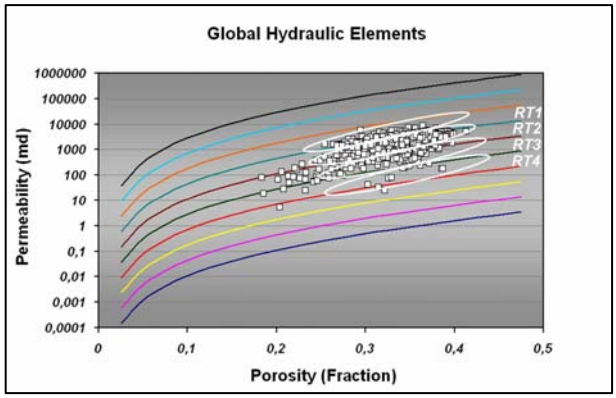

Figure 22. GHE Template / Rock Type Identification.

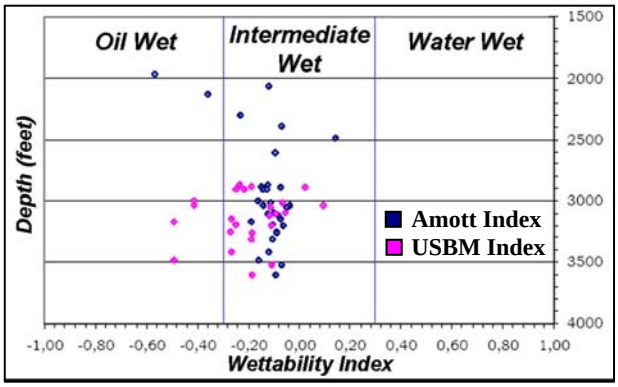

Figure 23. Wettability Index.

RT_GHE (adim)	RT_(SCAL) (adim)	Phi (fracc)	K (mD)	Swi (frac)	Sor (frac)	Sorg (frac)	FZI Prom (adim)
RT1	1	0.3089	2920	0.0265	0.3600	0.3670	6.81
	2	0.3530	4656	0.0702	0.3616	0.3550	6.59
	3	0.3260	3604	0.1077	0.3752	0.3790	6.81
RT2	4	0.3360	2944	0.1181	0.3742	0.3897	5.82
	5	0.3280	1667	0.1543	0.3028	0.4238	4.60
	6	0.3050	806	0.1927	0.2719	0.4494	3.69
RT3	7	0.2300	93	0.2796	0.2579	0.4974	2.11

Table 3. Rock Type Definition.

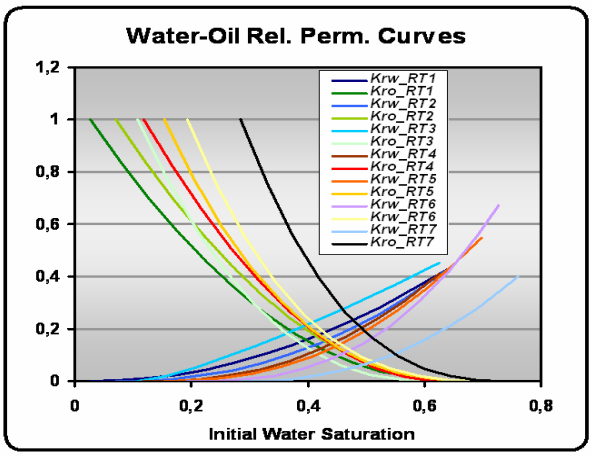

Figure 24. Water - Oil Relative Permeability Curves.

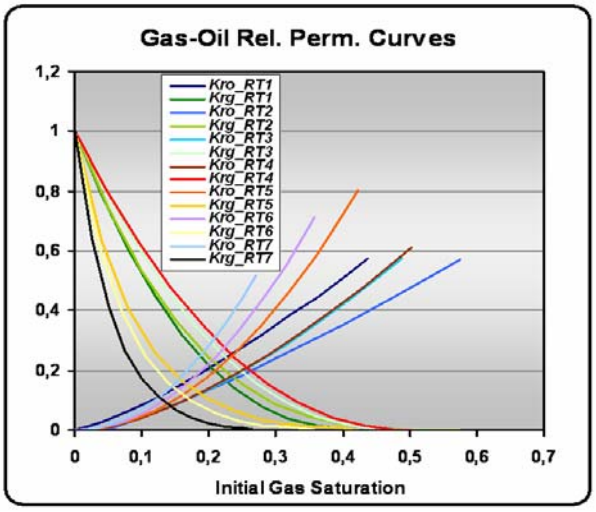

Figure 25. Gas - Oil Relative Permeability Curves.

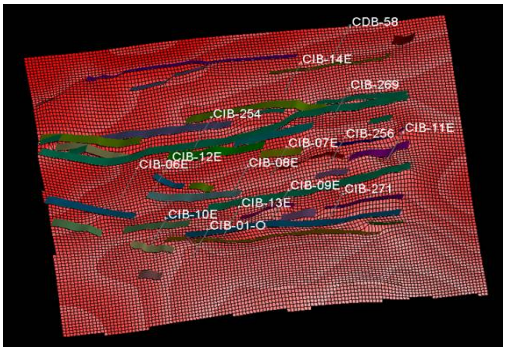

Figure 26. Static Pressure Data and Structural Framework.

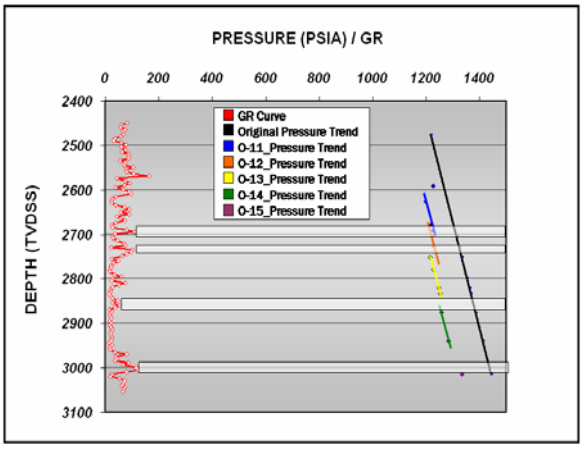

Figure 27. Static Pressure Data (Compartmentalization).

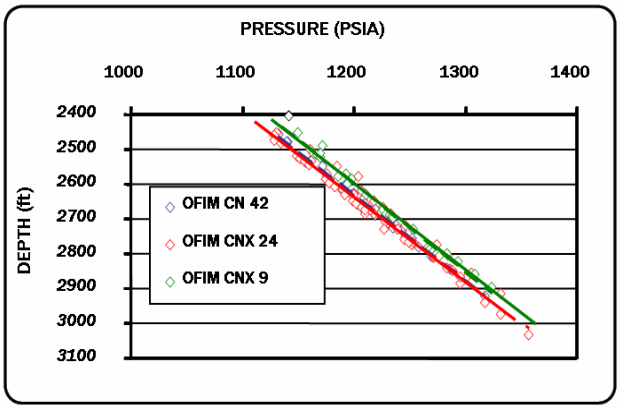

Figure 28. Static Pressure Trend Comparison.

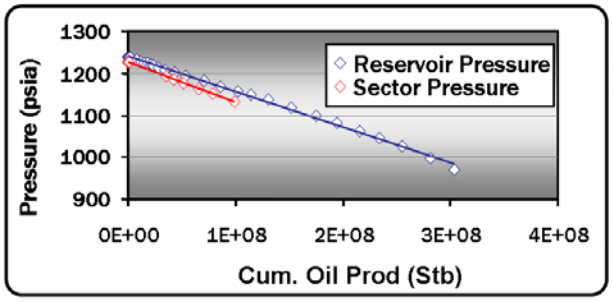

Figure 29. Pressure Model.

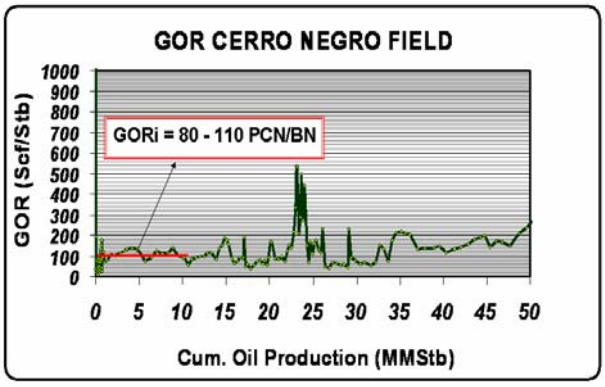

Figure 30. Initial Gas-Oil Ratio of Cerro Negro Field.

Year	Wells	T (°F)	GOR (Scf/Stb)	Sample	Analysis	Consistency	Validation
1980	CNX0007	111	29	Recombined	Conventional	NO	-
1980	CNX0009	127	40	Recombined	Conventional	NO	-
1980	CNX0014	116	39	Recombined	Conventional	NO	-
1980	CNX0015	116	71	Recombined	Conventional	NO	-
1980	CNX0018	100	54	Recombined	Conventional	NO	-
1981	CN0123	116	130	Recombined	Conventional	NO	-
1981	CNX0024	125	43	Recombined	Conventional	NO	-
1986	CH0026	124	80	Recombined	Conventional	NO	-
-	CO0004	126	79	Recombined	Conventional	NO	-
1981	CN0136	126	109	Recombined	Conventional	NO	-
1981	CNX0039	116	95	Recombined	Conventional	OK	NO
1981	CNX0042	122	84	Recombined	Conventional	OK	NO
1987	CD0006	122	98	Recombined	Conventional	OK	NO
1997	CI0210	129	100	Bottom	Conventional	NO	-
1997	CI0210	129	100	Bottom	Non-Conventional	NO	-
1997	CI0210	129	106	Recombined	Conventional	NO	-
1997	CI0210	129	107	Recombined	Non-Conventional	NO	-
2006	CIB0263	122	110	Recombined	Conventional	OK	NO

Table 4. PVT Samples of Cerro Negro Field.

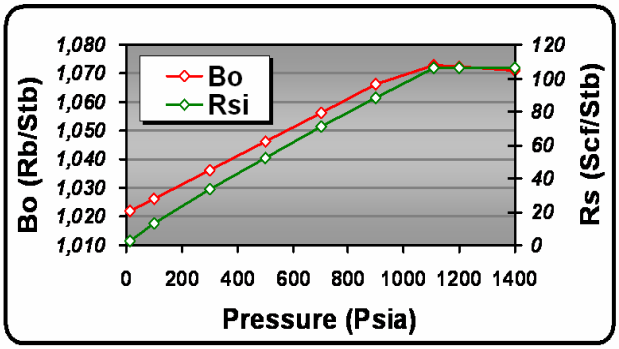

Figure 31. Oil Formation Volume Factor and Solution Gas to Oil Ratio.

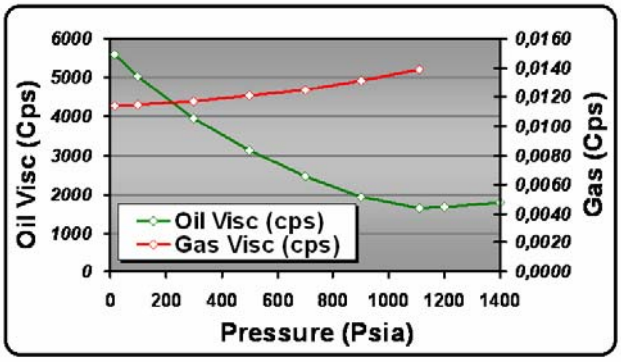

Figure 32. Gas and Oil Viscosities.

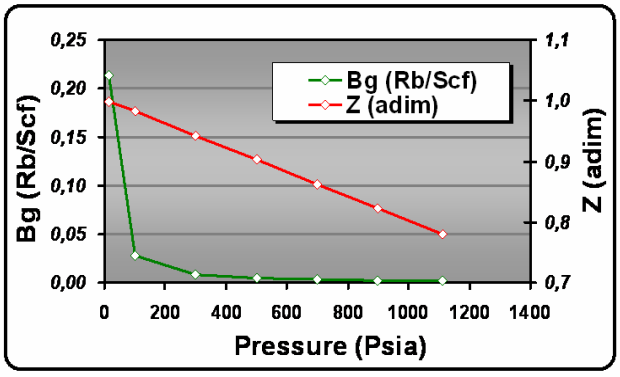

Figure 33. PVT Gas Properties.

Presión	Bw (Rb/Stb)	μw (Cps)	Cw (1/psia)
1200,00	1,0093	0,5822	2,874E-06
1110,00	1,0095	0,5799	2,879E-06
14,70	1,0110	0,5533	5,577E-03

Table 5. PVT Water Properties.

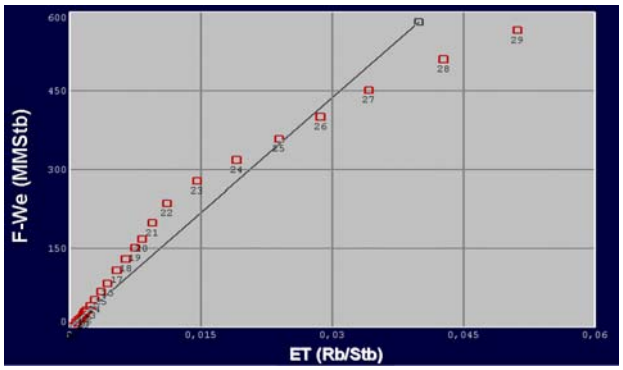

Figure 34. Havlena-Odeh / F-We Vs Et.

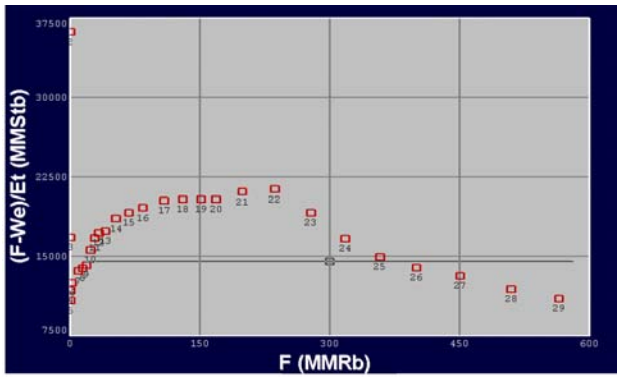

Figure 35. Campbell Plot.

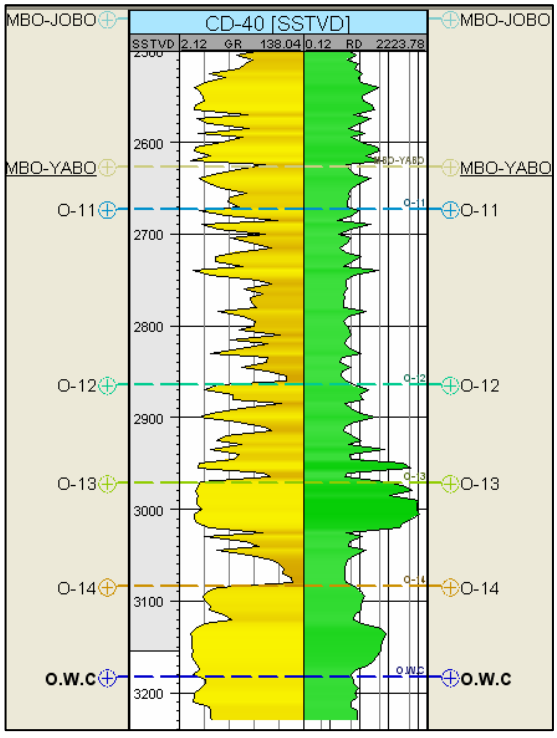

Figure 36. Oil Water Contact (CD-40).

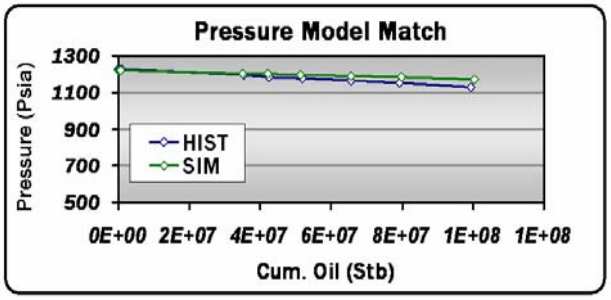

Figure 37. Pressure Match.

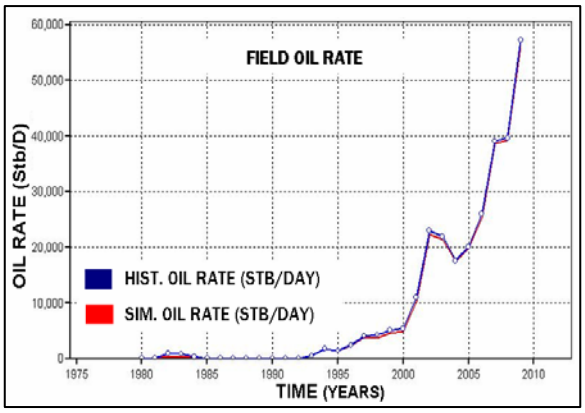

Figure 38. Oil Rate Match.

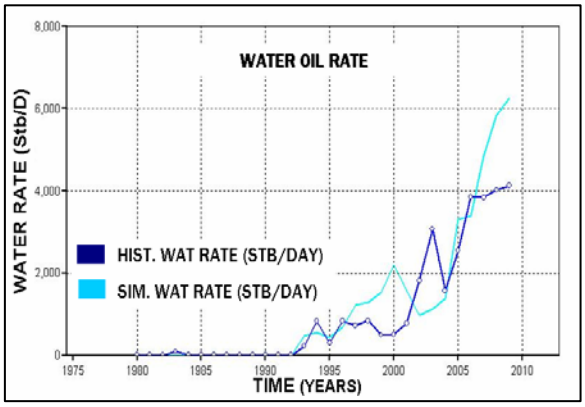

Figure 39. Water Rate Match.

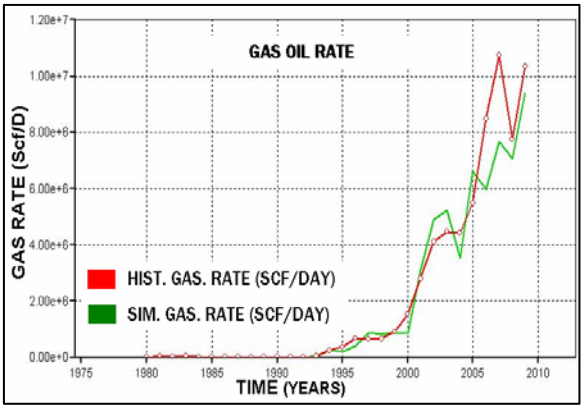

Figure 40. Gas Rate Match.

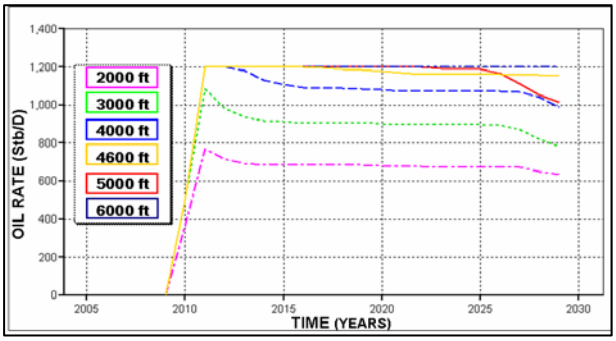

Figure 41. Oil Rate Comparison / Horizontal Length.

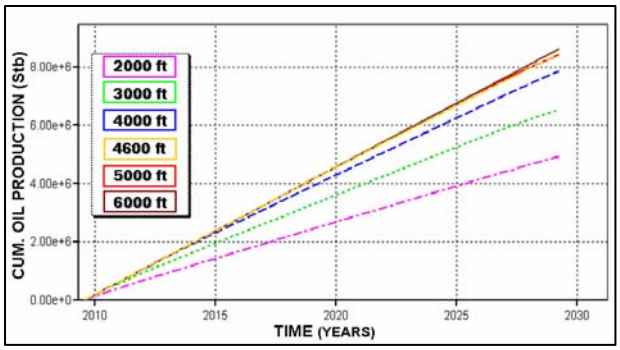

Figure 42. Cumulative Oil Production / Horizontal Length.

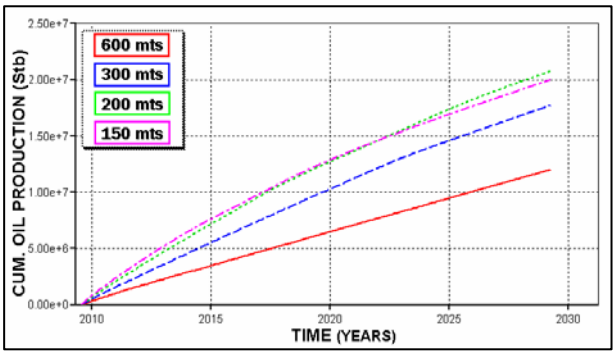

Figure 43. Cumulative Oil Production / Horizontal Spacing.

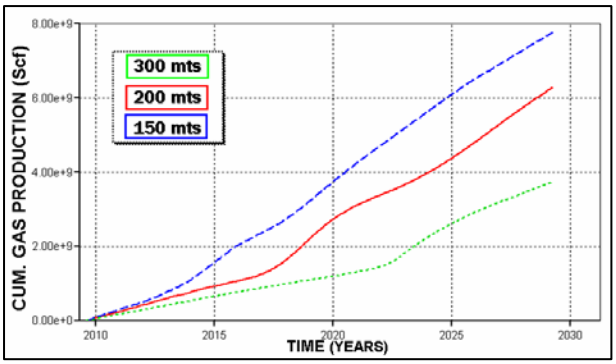

Figure 44. Cumulative Gas Production / Horizontal Spacing.

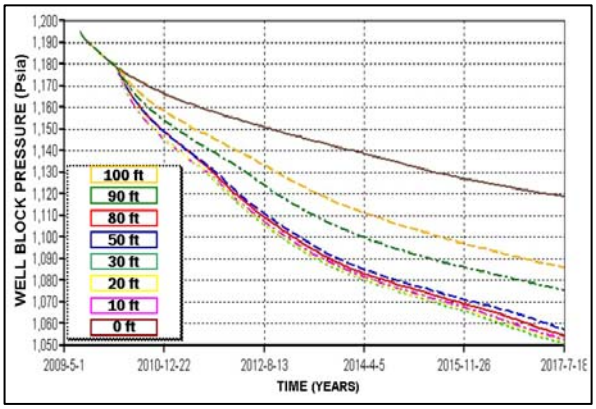

Figure 45. Static Pressure Vs Time / Vertical Spacing.

Figure 46. Base Case / Energetic Decline.

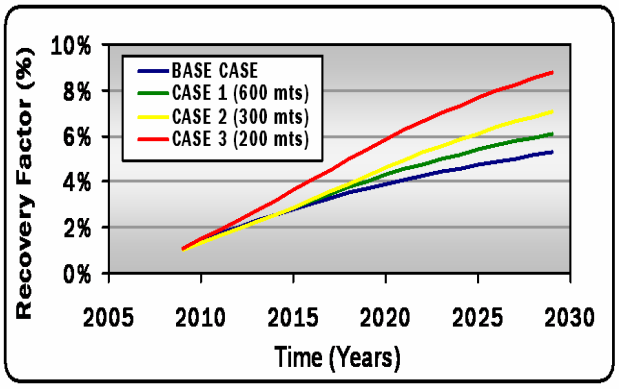

Figure 47. Forecast Results.